

A new class of erbium doped optical fiber for high power optical amplifier

Mukul Chandra Paul¹ · Mrinmay Pal¹ · Shyamal Das¹ · Anirban Dhar¹ · Shyamal K. Bhadra¹

Received: 24 December 2014 / Accepted: 22 September 2015 / Published online: 23 July 2016
© The Optical Society of India 2016

Abstract We report a new composition of optical fiber containing ZrO_2 to get better solubility of Er and Er/Yb for efficient high power optical amplifier. Performance of the doped fibers composed of zirconia–yttria–alumina–silica glass–ceramic host is studied for multi-wavelength-channel amplification in C-band region with core as well as cladding pumped configuration. The cross-section of the fibers is made almost hexagonal and coated with low index polymer acrylate resin. Maximum output power of 0.5 W is achieved at 1572 nm when I/P signal is maintained in the range +6 to 9 dBm at pump power of 4 W. This type of glass composition doped with Er shows 30 % pump conversion efficiency, however, there is a scope for improvement.

Keywords Erbium doped fiber · Glass–ceramic · Multichannel amplification and optical amplifier

Introduction

Recently high power optical amplifiers are demonstrated to meet the demand for various applications. Various materials are used as host for the erbium ions, such as silica, alumina, telluride, phosphate glass, and others [1–3]. In-depth studies have shown that different materials have different impacts on the performance of the developed waveguide or amplifier. Some materials allow higher erbium concentrations to be realized without the

detrimental effects of concentration quenching [4] and cluster formation [5], thereby providing higher gain for a compact device.

Erbium Doped Fiber (EDF) is generally not a cost-effective solution for high output (>27 dBm) applications due to the prohibitive cost of high power single mode pump lasers. To relax this limitation, a double-clad Erbium codoped with Ytterbium fiber (EYDF) amplifier is required in which the signal light propagates in the core and pump light propagates in the first cladding around the core. Such a double-clad EYDF amplifier can use watt-class multimode laser diodes, with a promise of realizing amplifier of high output power. Compared with EDF, the co-doping with Yb ions considerably improves the pump absorption. In EYDF, the ytterbium can absorb a pump photon within its spectral band of 800–1100 nm, and be excited to the $^2F_{5/2}$ state, from which it can transfer energy to $^4I_{11/2}$ state of erbium ion. The ions in $^4I_{11/2}$ then make a nonradiative transition to $^4I_{13/2}$, forming a population inversion between $^4I_{13/2}$ and $^4I_{15/2}$, thereby producing amplification of incident optical signal around 1550 nm.

In the quest of developing high power Er/Yb codoped fiber, Samson et al. [6] developed commercial grade fiber lasers and amplifiers of multiple hundred to kW level. Amongst others, Jebali et al. [7] also developed full range of Er/Yb doped fiber for wide range of optical amplifiers required for DWDM, CATV and other telecommunication applications. The global optical amplifier market was \$900 million in 2012, which is anticipated to reach \$2.8 billion by 2019 [8].

High-power eye-safe laser radiation in the spectral region between 1500 and 1700 nm is attractive for many applications, including free-space telecommunications, range finding, and remote sensing. An all-fiber format is of great interest outside the laboratory environment. Among

✉ Shyamal K. Bhadra
skbhadra@cgcric.res.in

¹ Fiber Optics and Photonics Division, CSIR-Central Glass and Ceramic Research Institute, Kolkata 700 032, India

single-mode fiber sources at these wavelengths, the highest output power of 150 W with 33 % efficiency was achieved using Er/Yb co-doped fibers cladding pumped at 915 or 976 nm [9]. However, for the maximum output power, amplified spontaneous emission from Yb ions at 1000 nm reaches 50 % of the laser power at 1560 nm, leading to a rollover of the slope efficiency and raising the difficult issue of getting rid of the parasitic (non-eye-safe) radiation. In recent past significant success has been made in power scaling of in-band pumped Er-doped fiber (EDF) lasers and amplifiers [10–13]. In such approach the reduced quantum defect leads to a very attractive lasing slope efficiency of 75 % [11]. However, the electrical to optical efficiency of the pump sources used (diodes or Er–Yb fiber lasers at 1532 nm [10, 11] and Raman fiber lasers at 1480 nm [12] is at least two times lower than that of usual pump diodes at 976 nm, making the overall electrical- to-optical efficiency in in-band pumped lasers lower than 15 %.

It appears that the double-clad (DC) Yb-free EDF pumped at 976 nm is the simplest architecture. Slope efficiencies of 24 % [14] in a single-mode fiber and 30 % [15] in a multimode fiber have been reported. By decreasing the pump-cladding diameter and using suitable core glass matrix, a slope efficiency of 32 % (>7 W at 1575 nm with potential power scaling) in a single-mode EDF [16] has been demonstrated. Very recently Kotov et al. [17] demonstrated 75 W 40 % efficiency single-mode all-fiber erbium-doped laser cladding pumped at 976 nm.

In order to augment the power scale, a new class of cladding pumped fiber is necessary and the complete packaging with the pump laser source is a challenging task. Since the demand for high power erbium or erbium-ytterbium doped optical amplifier (HP-EDFA and HP-EYDFA) is increasing we tried to look into the possibility of getting new composition of glass host for efficient amplification.

The composition of the doping host should be engineered properly for reducing the clustering effect of Er or ErYb ions. A new type of erbium-doped fiber (EDF) having core glass compositions of zirconia–yttria–alumina–phospho-silica glass is fabricated where a high erbium doping concentration >4000 ppm without any phase separations of dopants can be achieved. Brasse et al. [18] studied the luminescence properties of erbium and ytterbium doped silica–zirconia nanostructured optical fibers prepared by the chemical sol–gel method. Here we tried to fabricate the doped fibers using MCVD process with solution doping technique under certain special conditions. Experiments for core and cladding pumped of asymmetric fiber structure for high power amplifiers are carried out and results appeared to be encouraging for efficient amplification.

Experimental procedure

Optical preforms based on zirconia–yttria–alumina–phospho silica glass (Zr–Y–Al–EDF) using modified chemical vapour deposition (MCVD) process in combination with solution doping technique are fabricated. Details are reported elsewhere [19]. The doping of Er_2O_3 into the host is done via solution doping process. Small amounts of Y_2O_3 and P_2O_5 are added at this stage to serve as nucleating agent. This step is necessary to increase the phase separation for generating Er_2O_3 doped micro crystallites in the core matrix of the optical preform [19–21]. The glass formers incorporated by the MCVD process are SiO_2 and P_2O_5 along with the glass modifiers Al_2O_3 , ZrO_2 , Er_2O_3 and Y_2O_3 , which are incorporated by the solution doping technique using an alcohol-water mixture of suitable strength (1:5) to form the complex molecules $\text{ErCl}_3 \cdot 6\text{H}_2\text{O}$, $\text{AlCl}_3 \cdot 6\text{H}_2\text{O}$, $\text{YCl}_3 \cdot 6\text{H}_2\text{O}$ and $\text{ZrOCl}_2 \cdot 8\text{H}_2\text{O}$. Figure 1a shows the deposition of porous phospho-silica layer inside the pure silica substrate tube, while Fig. 1b shows the actual collapsing process in MCVD set-up. The inclusion of the Y_2O_3 particulates into the host matrix serves the additional purpose of slowing down or eliminating changes in the ZrO_2 crystal structure. This is a crucial factor in the fabrication process. Pure zirconium dioxide can exist in three distinct crystalline states in bulk glass matrix, depending on the fabrication temperature as described earlier [19–21]. It can be seen that ZrO_2 crystallites are able to sustain their crystalline structures at elevated temperatures above which it collapses to form preform under certain conditions and later we draw the fiber from the preform of desired dimension and length.

In an intermediate stage, the preform was annealed at 1100 °C for 3 h in a closed furnace under heating and cooling rates of 20 °C/min to generate Er_2O_3 -doped ZrO_2 rich nano-crystalline particles and subsequently fibers were drawn with on-line resin coating using fiber drawing tower. Details of such three fibers are given in Table 1.

At fiber drawing temperature of around 2000 °C, the nano-crystalline host of ZrO_2 was preserved in the silica glass matrix as confirmed by the TEM analyses with EDX spectra and electron diffraction patterns as shown in Fig. 2. Therefore it could be ascertained that during fiber drawing at high temperature further vitrification could be avoided. This clearly confirms the existence of ZrO_2 crystallites within the host matrix of the preform.

The average particle sizes are in the range 5–8 nm. The core and cladding geometry of the fiber was inspected by high resolution optical microscope (Olympus BX51). The core was homogeneous and had no observable defects at the interface between the core and the silica cladding. The average dopant percentages of the fiber preform samples

Fig. 1 **a** Deposition of porous phospho-silica layer inside the silica substrate tube and **b** collapsing is in progress for making Zr-EDF preform

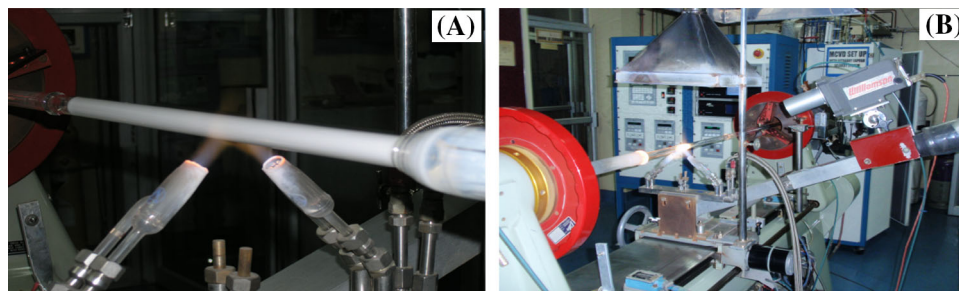
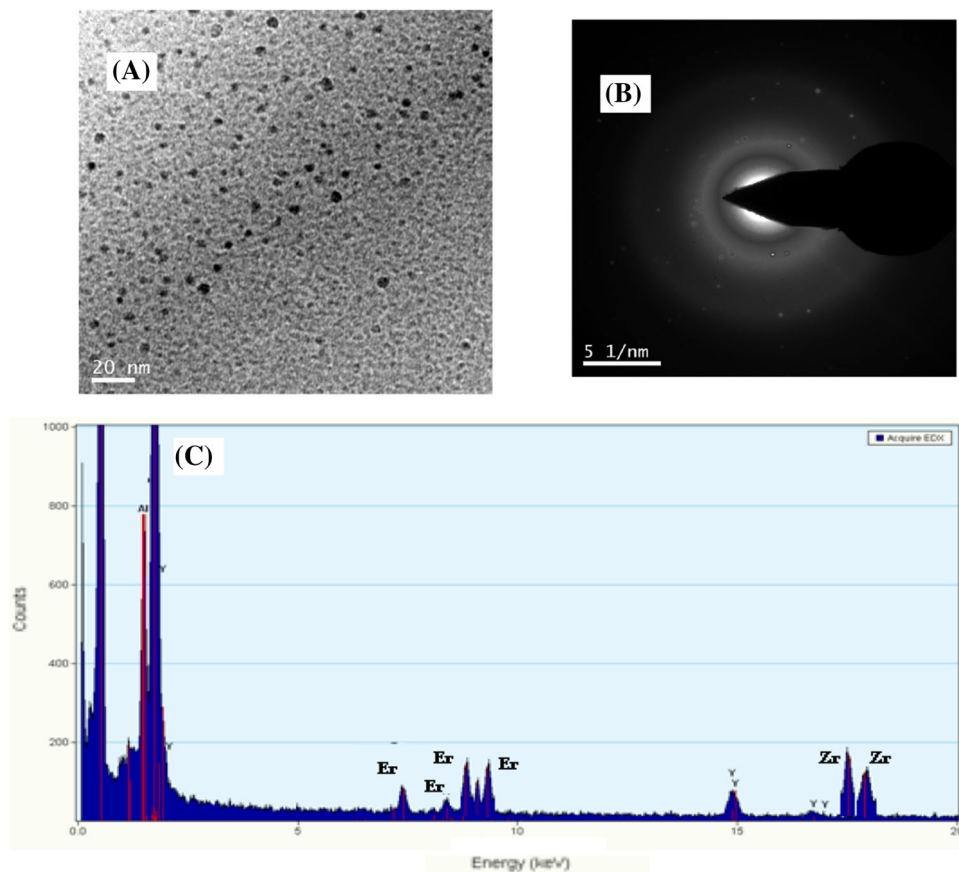


Table 1 Nano-crystalline zirconia yttria alumina silica particles doped optical fibers

Fiber No	Composition of doping host	NA	Core diameter (μm)	Er ion concentration (ppm wt)
MEr-1	$\text{SiO}_2\text{-Al}_2\text{O}_3\text{-Y}_2\text{O}_3\text{-ZrO}_2\text{-P}_2\text{O}_5\text{-Er}_2\text{O}_3$	0.17	10.5	2800
MEr-2	$\text{SiO}_2\text{-Al}_2\text{O}_3\text{-Y}_2\text{O}_3\text{-ZrO}_2\text{-P}_2\text{O}_5\text{-Er}_2\text{O}_3$	0.19	10.0	3888
MEr-3	$\text{SiO}_2\text{-Al}_2\text{O}_3\text{-Y}_2\text{O}_3\text{-ZrO}_2\text{-P}_2\text{O}_5\text{-Er}_2\text{O}_3$	0.21	10.3	4320

Fig. 2 **a** TEM image of fiber core glass shows nano-crystallites-black spots, **b** electron diffraction pattern of nano particle of Zr-EDF (MEr-2) and **c** EDX analyses showing presence of Er Y, Al and Zr



were measured by electron probe microanalyses (EPMA) as shown in Table 2.

Three different types of nano-engineered glass based Zr-EDFs were fabricated with variation of the doping levels of different co-dopants. The cross-sectional view of one of the

fabricated Zr-EDF (MEr-2) is shown in Fig. 3a. It can be seen that it does not contain any core-clad imperfection which may affect bending loss of the fiber. The refractive-index profile of fiber (MEr-1) is shown in Fig. 3b. The spectral attenuation curve of fiber MEr-2, is shown in

Table 2 Doping levels within core region of the preforms

Preform No	Al ₂ O ₃ (mole %)	ZrO ₂ (mole %)	Er ₂ O ₃ (mole %)
MEr-1	0.25	0.65	0.155
MEr-2	0.26	1.47	0.195
MEr-3	0.24	2.10	0.225

Fig. 3c. The Zr-EDFs show small variation of the fluorescence lifetime at different pump powers varying from 50 to 300 mW.

Their fluorescence lifetimes are observed to be around 8 and 10 ms under 100 mw pump power at 976 nm wavelength. MEr-1 shows a slightly lower fluorescence lifetime of around 8.0 ms as the fiber contains low doping level of ZrO₂. With a combination of both Zr and Al along with other co-dopants, we achieved high erbium concentration of 4320 ppm in the fiber MEr-3 without any phase separations and concentration quenching effect of RE elements. One of the conventional methods to test for quenching is the measurement of fluorescence lifetime of Er ions at different pump powers. There must be concentration quenching of Er ions, if the fluorescence lifetime differs too much with different pump power [22]. In order to check this property we have measured the fluorescence lifetime of two different doped EDF hosts at different pump powers as shown in Fig. 4. The curves show that there was not much noticeable change of measured lifetime of Zr-EDF (MEr-3) that only changes from 10.65 to 10.70 ms with increasing pump power from 25 to 250 mW (Fig. 4). This confirms favourably to the lifetime of alumina-silica glass based EDF that normally varies from 10.25 to 10.58 ms. This phenomenon indicates that nano-crystalline ZrO₂ prevents the formation of Er–Er bonds which reduces the quenching process of Er ions even at high doping levels of around 4320 ppm. The success is related to co-doping of ZrO₂ with Al₂O₃. Both aluminium and zirconium ions surround

the Er ions form a solvation shell thereby adjusting the charge balance and improving the solubility of Er ions into the host. This inhibits clustering of the Er ions.

We have experimented simultaneous four-channel amplification at different input signal levels (20, 25 and 30 dBm/ch) at different pump powers (40, 50, and 60 mW) using one of the Zr-EDFs (MEr-3) details described recently [21]. The amplified signals and output SNRs were measured for three different pump powers of 40, 50 and 60 mW at 20 dBm/ch input signal level. Signal amplifications were increased in each channel and it was more rapid in the shorter wavelength side of C-band as pump power was increased, and the output SNRs are always >31 dB for each channel [21]. The nature of signal amplifications and SNRs were measured for three different input signal levels (–20, –25 and –30 dBm/ch) for constant pump power of 50 mW [21]. It is observed that there is appreciable optical gain of at least 20 dB for –20 dBm/ch and a minimum output SNR of 21.8 dB for 30 dBm/ch input signal levels. Both the gain and output SNRs would

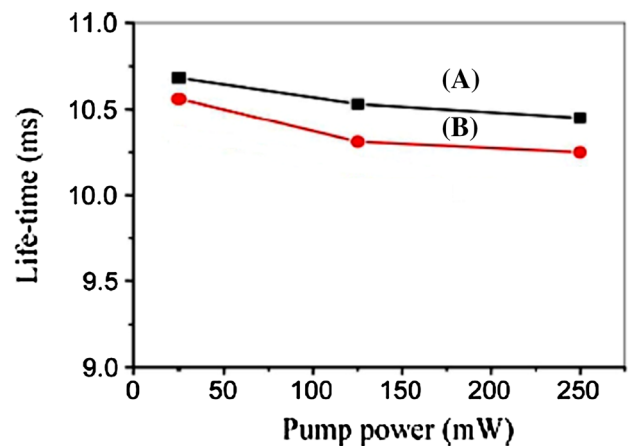


Fig. 4 Fluorescence lifetime of three EDFs. **a** MEr-3 and **b** alumina-silica glass based EDF at different pump powers

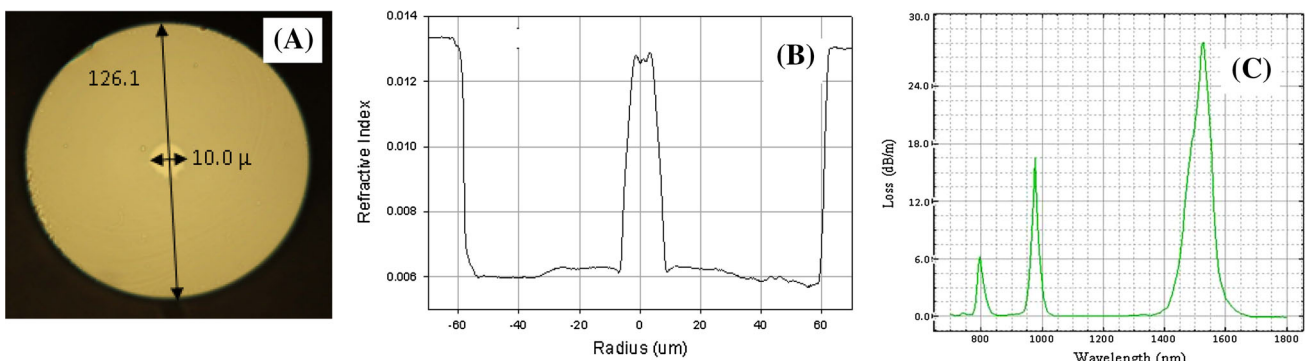


Fig. 3 **a** Cross-sectional view (MEr-2), **b** refractive index profile (MEr-1) and **c** loss curve of EDF (MEr-2)

increase if pump power was further increased. The measured noise figures were within 4.2–4.7 dB. The critical passive losses of erbium doped optical fiber in EDFA system arises from OH-absorption that is present in doped glass which gives rise to strong absorption at 1380 nm wavelength. The presence of OH degrades the gain performance of the fibers due to the energy transfer from $^4I_{13/2}$ level to OH ions. The OH absorption losses of all the three fibers at 1380 nm wavelength are kept within 200–250 dB/Km. On the other hand, splicing losses with standard SMF-28 fiber induces further loss in EDFA system which also reduces the pump efficiency of the fiber. All the splicing losses of all the three fibers should be 0.04–0.05 dB for better performance.

The experimental results show that the Zr-EDF (MEr-3) is quite suitable for multichannel small-signal amplification. In our experiment, we targeted the minimum gain of 22.5 ± 0.5 dB for input signal level of -30 dBm/ch. The length of the fiber used in the experiment was 1.5 m. The measured results of output power and SNR is shown in Fig. 5. We obtained gain difference (max-to-min gain) of less than 2 dB in MEr-3 sample.

The maximum noise level was -28.5 dBm/nm for MEr-3. Moreover, MEr-3 showed an output SNR value of >22 dB. The motivation for choosing nanocrystalline zirconia dispersed into silica glass matrix is to get low noise as well as better flatness of the gain spectrum at high doping level of Er ions. ZrO_2 is well known for its outstanding chemical and physical properties like superior hardness, chemical stability, and thermomechanical resistance. Due to its optical transparency, high refractive index, and photochemical stability, ZrO_2 is an excellent candidate for photonic applications. A major factor that influences quenching process in rare-earth-doped materials is multiphonon relaxation. Zirconium oxide possesses a stretching vibration at about 470 cm^{-1} , which is very low compared with that of Al_2O_3 (870 cm^{-1}) and SiO_2

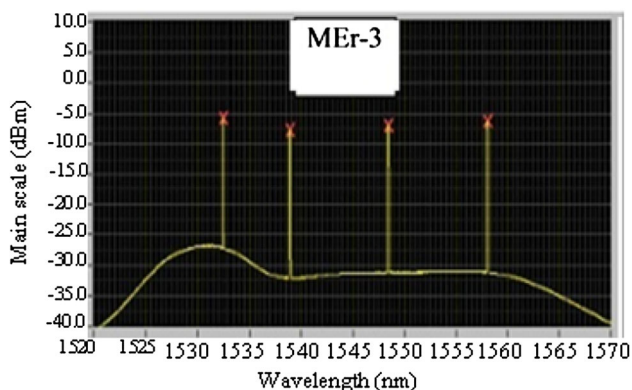


Fig. 5 Four-channel amplification in MEr-3. Input signal level: -30 dBm/ch

(1100 cm^{-1}). Hence, much attention is given to select such host materials with low phonon energy in order to improve the erbium ion solubility with reduced concentration quenching process and enhance the gain flatness and output SNRs for multichannel small-signal amplification. Next we will discuss high power EDFA in cladding pump configuration.

EDF for high power optical amplifier

As stated earlier the composition of the doping host should be engineered properly for reducing the clustering effect of Er ions. We have tried to develop new compositional of glass host for doping of Er ions with high ZrO_2 content with large cladding pump region. The microscopic image of hexagonal shaped low RI coated erbium doped fiber (HPE-2), core and cladding spectral absorption curves are shown in Fig. 6a–c. The core absorption is around 80 dB/m at 980 nm wavelength whereas cladding absorption is around 2.0 dB/m at 980 nm. The different dopants are distributed uniformly along the diameter of the fiber, which is confirmed by electron probe micro-analysis (EPMA) as shown in Fig. 7a. A preliminary result of optical amplification using 4 m length of fiber under 4 W pump power having I/P signal in the range $+6$ to 9 dBm is shown in Fig. 7b. The wideband ASE is observed for the yttria stabilized zirconia-alumina-phospho-silica glass host with hexagonal shaped cladding structure coated with low RI resin under different cladding pump power is given in Fig. 8. The experiment is carried out at CSIR-CGCRI. The maximum 0.5 W output power at 1572 nm is achieved with high doping of erbium under launched pump power of 4 W having high input signal power of $+6$ to 9 dBm. Based on the results the calculated maximum pump conversion efficiency is found to be 30 %.

A wide band emission from 1530 to 1620 nm is observed. As zirconium oxide has a stretching vibration at about 470 cm^{-1} , which is very low compared to that of Al_2O_3 (870 cm^{-1}) and SiO_2 (1100 cm^{-1}) [23], partially crystalline zirconia rich erbium oxide phase-separated particles possesses lower phonon energy which gives rise to increase of larger emission cross section [21]. The introduction of Zr^{4+} allows one to avoid formation of Er^{3+} clusters in silica host and consequently to make it more intense luminescence [19]. Replacement of the intermediate Al_2O_3 by a modifier ZrO_2 , the number of non-bridging oxygen is expected to increase which makes the silica network structure more open. As a result, Zr-EDF has wider emission spectra as compared to silica-EDF, especially at the longer wavelengths around 1600 nm because of its larger emission cross-section [19, 20].

The widening of the ASE spectra towards longer wavelength is believed to be a result of the Stark level of

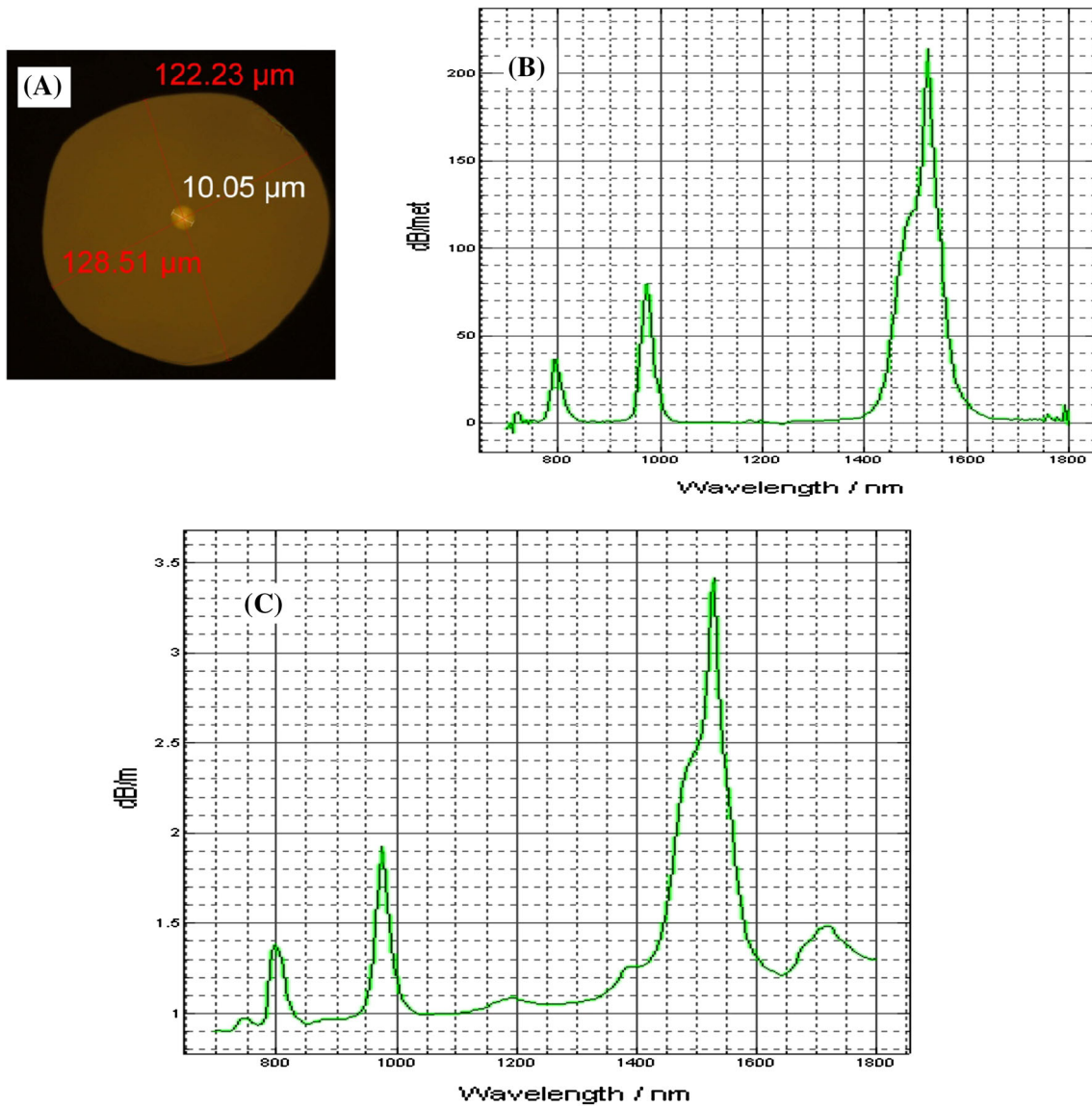


Fig. 6 Cross-sectional view (a), core absorption loss (b) and cladding absorption loss (c) of high concentration of Erbium doped fiber (HPE-2)

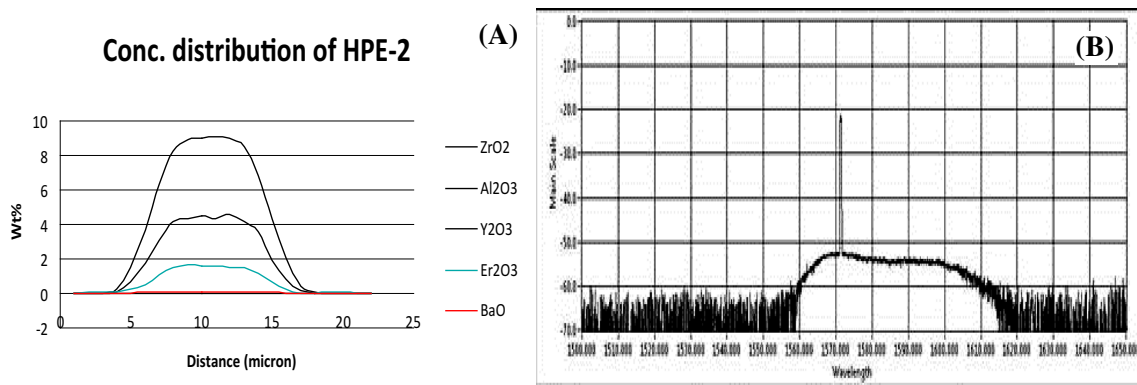


Fig. 7 a Distribution of different dopants across the core diameter and b amplification curve of EDF (HPE-2) under 4 W pump power at 980 nm having I/P Signal +6 to 9 dBm with O/P signal of 500 mW

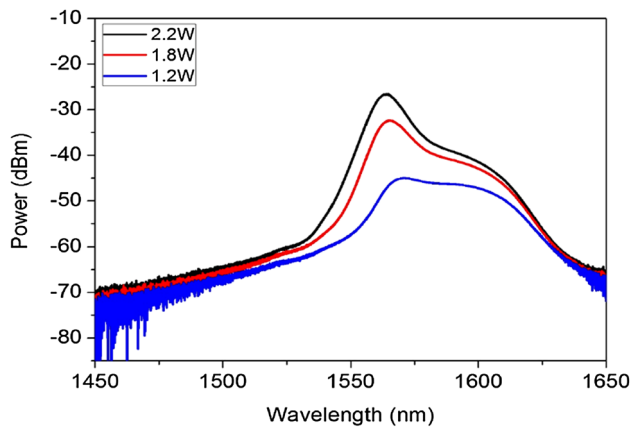


Fig. 8 ASE output for 6 m HPEr-5 for different pump power in the wavelength range (1450–1650 nm)

the Er^{3+} ions in the Zr-EDF, which is separated to a larger degree due to intense ligand field. This is due to inhomogeneous energy level degeneracy that the ligand field of the Zirconia host glass induced as a result of site-to-site variation causing the wide band optical transitions.

To make a cost effective solution, a double-clad Erbium co-doped with Ytterbium fiber (EYDF) amplifier is required in which the signal light propagates in the core and pump light propagates in the first cladding around the core. In EYDF, compared with EDF, the co-doping with Yb ions considerably improves the pump absorption.

We try to develop zirconia-alumina-phospho silica glass based Er–Yb codoped fiber for high power optical amplifier having output signal power above +40 dBm. The hexagonal shaped structure of preform along with cross-sectional view of fiber drawn from such preform is shown in Fig. 9a, b respectively. Distribution of different dopants along the core diameter of one such sample fiber is shown in Fig. 9c. P_2O_5 is evaporated partly during the collapsing stage as a result a dip is observed around the central core region. This type of low RI coated hexagonal cladding shaped Er/Yb codoped fiber shows core absorption of 75 dB/m at 1550 nm and cladding absorption of 1.5 dB/m at 915 nm with NA around 0.12 and core diameter of 11.5 μ . Detail study on the lasing properties is in progress.

If the asymmetric structure of cladding is not ideal, slightly shifting of the core gives rise to splicing problem showing higher splicing loss during splicing of EDF with other components. The snap shots of a specially designed splicing machine (Fig. 10) show the splicing loss of around 1.47 dB of hexagonal shaped cladding structure with shifting of the core around 1.15 μ from the center position.

In a non-circular-shaped cladding the helical rays are coupled to the meridional rays and all pump light pass through the core. In both D-shaped and rectangular shaped clad structure provide pump absorption almost one

order of magnitude higher than that circular clad structure. NA of the pump cladding should be as high as possible to capture as much of the high-divergence pump light as possible. High NA around 0.4 can be achieved using low RI resin.

Some important observations

To reduce the non-linearity the fiber core requires larger size with low NA and uniform Er-distribution in the core glass. Also to inhibits concentration quenching it requires suitable host to enhance the solubility of rare-earths as RE solubility limit is few 100 ppm in SiO_2 and ~ 1000 ppm in $\text{SiO}_2\text{--Al}_2\text{O}_3$ glass. Co-doping with Yb ion restricts pair induced quenching effect which needs optimum selection of Er:Yb ratio and glass composition. Each surface of asymmetric structure of preform should be highly polished to prevent the formation of any scattering centers before fiber drawing. Optimization of fiber drawing parameters such as drawing tension and drawing temperature to maintain perfect hexagonal/octagonal cladding structure are extremely important. Reliability of polymer cladding under high optical power is also very essential for long term operation. Polymer materials are not as transparent as glass and will never be as environmentally stable as glass or metal.

To reduce the splicing loss, the asymmetric structure of silica cladding should be as much closer to the circular geometry. In this context octagonal cladding structure should be the best choice from the view point of low splicing loss. To make perfect octagonal shaped structure grinding and polishing of the circular preform should be done properly so that the core becomes at the central position with respect to each arm of an octagon. It is necessary to know how much grinding length will be require from each side with respect to initial diameter of preform for getting the perfect octagonal shaped structure with equal arm. All sides should be equal length placed around a common center so that all angles between the sides are also equal. We derived the following curves shown in Fig. 11 to get some initial idea about the grinding length from the circumference, length of each arm and distance between two opposite flat surface with respect to initial diameter of preform for making of perfect octagonal shaped preform. Finally when fiber is drawn from such perfect octagonal shaped preform, sharp edge of each vertex of an octagon will be slightly curved due to drawing tension into the octagonal shaped structure of the fiber.

Fig. 9 **a** Microscopic view of hexagonal shaped preform, **b** cross-section view of low RI coated hexagonal cladding shaped fiber (HEY-1) and **c** dopant distribution along the cross section of fiber sample

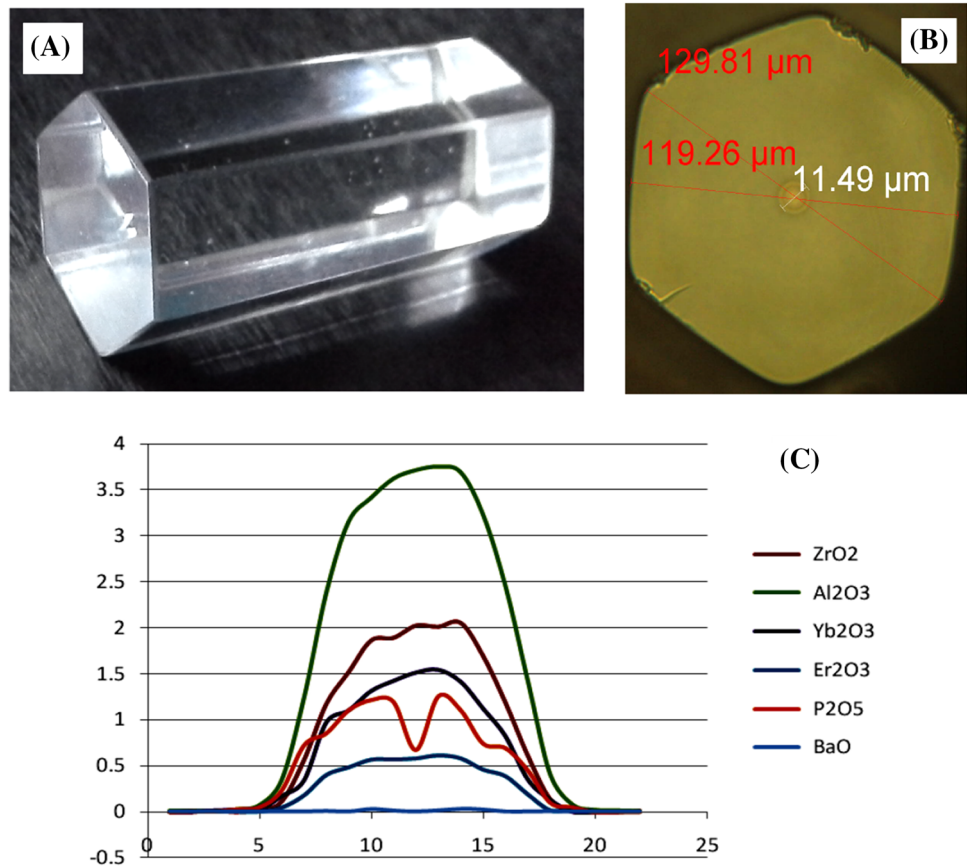


Fig. 10 Picture showing the core mismatch between passive and Hexagonal shaped low RI coated fiber with the splicing loss 01.47 dB

Conclusion

A special type erbium doped crystalline zirconia yttria alumina phospho silica based optical fiber is developed through solution doping technique followed by MCVD process with optimization of the process parameters at different stages of fabrication. Glass modifiers and nucleating agents are added into the host glass through proper annealing of the preform to generate uniform distribution of crystalline zirconia yttria alumina-phospho silica nanoparticles in the core region of optical fiber. Such new type

of Zr-EDF was analysed as multichannel amplification in C-band region. This particular fiber exhibits maximum gain difference <2 dB with output SNR of >22 dB at input signal level of -30 dBm/channel amplification under pumping at 980 nm wavelength. Using such kind of glass-ceramic based high erbium doped low RI coated hexagonal cladding shaped fiber having core absorption of 80 dB/m at 980 nm achieved 0.5 W output power at 1572 nm under 4 W pump power at 980 nm with I/P signal +6 to 9 dBm. The pump conversion efficiency obtained maximum 30 %. We have developed Er/Yb codoped fiber using similar host

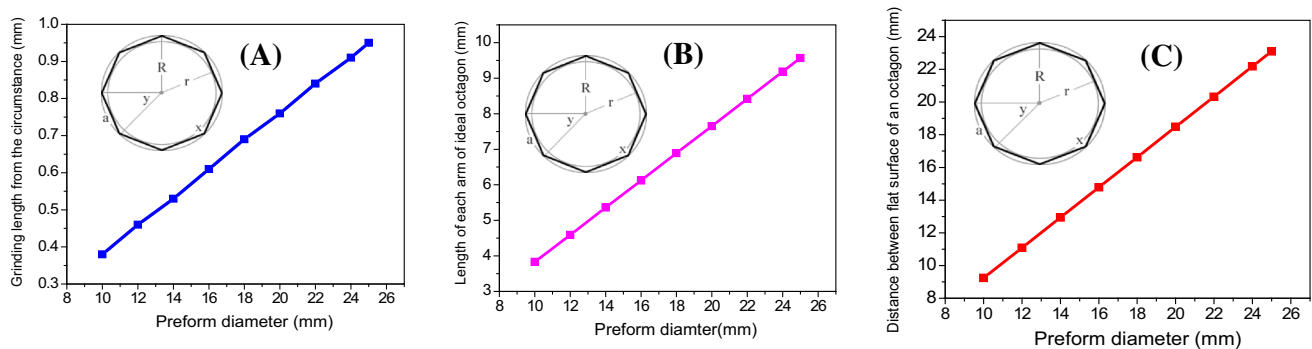


Fig. 11 **a** Grinding length versus preform diameter, **b** length of each arm versus preform diameter and **c** distance between two opposite flat surface versus preform diameter curves for making of ideal octagonal shaped structure of preform

glass with nano-crystallites to increase the pump conversion efficiency for making of high power optical amplifier.

Acknowledgement The authors are thankful to Director, CGCRI for his continuous encouragement, guidance and support in this work. Authors acknowledge with thanks the financial assistance from CSIR, Govt. of India. They are greatly obliged to Professor Jayanta Sahu, ORC, Southampton University, for his unstinted cooperation. Authors wish to thank SEM/ESCA Laboratory, CGCRI for SEM analyses of the samples. Authors are grateful to Centro de Investigaciones en Optica, Guanajuato, Mexico for measurement of fluorescence lifetime of different EDFs. They also are indebted to the staff members of FOPD, CGCRI for their sincere help.

References

1. M. Naftaly, S. Shen, A. Jha, *J. Appl. Opt.* **39**, 4979–4984 (2000)
2. S. Jiang, B.-C. Hwang, T. Luo, K. Seneschal, F. Smektala, S. Honkanen, J. Lucas, N. Peyghambarian, in *Optical Fiber Communications Conference Proceedings, PD5-1* (2000)
3. S.W. Harun, R. Parvizi, X.S. Cheng, A. Parvizi, S.D. Emami, H. Arof, H. Ahmad, *Opt. Laser Technol.* **42**, 790–793 (2010)
4. E. Snoeks, P.G. Kik, A. Polman, *E. Opt. Mater.* **5**, 159–167 (1996)
5. D.M. Gill, L. McCaughan, J.C. Wright, *Phys. Rev. B* **53**, 2334–2344 (1996)
6. B. Samson, G. Frith, A. Carter, K. Tankala, in *Optical Fiber Communication Conference and Exposition and the National Fiber Optic Engineers Conference, OSA Technical Digest (CD), paper OTuJ6* (2008)
7. M.A. Jebali, J.-N. Maran, S. LaRochelle, *Opt. Lett.* **39**(13), 3974 (2014)
8. New York, 30 Jan 2013 /PRNewswire/—www.Reportlinker.com
9. Y. Jeong, J.K. Sahu, D.B.S. Soh, C.A. Codemard, J. Nilsson, *Opt. Lett.* **30**, 2997 (2005)
10. J. Zhang, V. Fromzel, M. Dubinskii, *Opt. Express* **19**, 5574 (2011)
11. M.A. Jebali, J. Maran, S. LaRochelle, S. Chatigny, M. Lapointe, E. Gagnon, in *Conference on Lasers and Electro-Optics 2012: A&T, paper JTh11* (Optical Society of America, 2012)
12. V.R. Supradeepa, J.W. Nicholson, K. Feder, in *Conference on Lasers and Electro-Optics 2012: S&I, paper CM2N* (Optical Society of America, 2012)
13. E.-L. Lim, S.-U. Alam, D.J. Richardson, *Opt. Express* **20**, 13886 (2012)
14. V. Kuhn, D. Kracht, J. Neumann, P. Wessels, in *CLEO/Europe and EQEC 2011 Conference Digest, paper CJ7_5* (Optical Society of America, 2011)
15. V. Kuhn, D. Kracht, J. Neumann, P. Wessels, *IEEE Photon. Technol. Lett.* **23**, 432 (2011)
16. L.V. Kotov, M.E. Likhachev, M.M. Bubnov, O.I. Medvedkov, D.S. Lipatov, N.N. Vechkanov, A.N. Guryanov, *Quantum Electron.* **42**, 432 (2012)
17. L.V. Kotov, M.E. Likhachev, M.M. Bubnov, O.I. Medvedkov, M.V. Yashkov, A.N. Guryanov, J. Lhermite, S. Février, E. Cormier, *Opt. Lett.* **38**(13), 2230 (2013)
18. G. Brasse, C. Restoin, Y. Ouerdane, P. Roy, J.-M. Blondy, *J. Lumin.* **131**, 2427–2431 (2011)
19. M.C. Paul, S.W. Harun, N.A.D. Huri, A. Hamzah, S. Das, M. Pal, S.K. Bhadra, H. Ahmad, S. Yoo, M.P. Kalita, A.J. Boyland, J.K. Sahu, *J. Lightwave Technol.* **28**, 2919–2924 (2011)
20. M.C. Paul, S.W. Harun, N.A.D. Huri, A. Hamzah, S. Das, M. Pal, S.K. Bhadra, H. Ahmad, S. Yoo, M.P. Kalita, A.J. Boyland, J.K. Sahu, *Opt. Lett.* **35**, 2882–2884 (2010)
21. M. Pal, M.C. Paul, S.K. Bhadra, S. Das, S. Yoo, M.P. Kalita, A.J. Boyland, J.K. Sahu, *J. Lightwave Technol.* **29**, 2110–2115 (2011)
22. K. Aiso, Y. Tashiro, T. Suzuki, T. Yagi, *Furukawa Rev.* **20**, 41–45 (2001)
23. A. Patra, C.S. Friend, R. Kapoor, P.N. Prasad, *J. Phys. Chem. B* **106**(8), 1909–1912 (2002)